

STRESS-STRAIN STATE OF AN ICE SHEET SUBJECTED TO A MOVING LOAD UNDER SHALLOW-WATER CONDITIONS

V. D. Zhestkaya

UDC 532.526.2

The following two classes of problems of determining the stress-strain state of an ice sheet under a moving load are considered: determination of the resonant velocity for a load moving over a continuous ice field and calculation of the deflections of an ice field with a bounded ice-free zone subjected to a moving load. The problems are solved in a dynamic formulation. The algorithm of solution is based on the finite-element method and finite-difference methods. Examples of calculations are given.

The necessity of ice breaking can arise in navigation and in the operation of engineering structures in river and seawater areas in spring, autumn, and winter. For this purpose, the resonant method of ice breaking [1] realized by means of an air-cushion ship (ACS) can be used. In this case, the main parameters of motion of the ship (velocity and trajectory of motion) for which ice breaking is most efficient from the viewpoint of the expenditure of energy must be specified. The main specific features that occur in this case can be estimated by the method proposed by the author [2]. This method is based on the equation of viscoelastic vibrations of ice under the action of a moving load [3]

$$D\left(1 + \tau_f \frac{\partial}{\partial t}\right) \nabla^4 w + \rho_w g w + \rho_i h \frac{\partial^2 w}{\partial t^2} + \rho_w \frac{\partial \Phi}{\partial t} \Big|_{z=0} = p(t),$$

the Laplace equation for the function Φ , and the boundary conditions at the bottom of a basin and the ice-water interface

$$\frac{\partial \Phi}{\partial z} \Big|_{z=-H} = 0, \quad \frac{\partial w}{\partial t} - \frac{\partial \Phi}{\partial z} \Big|_{z=0} = 0,$$

where D is the flexural rigidity of the plate, τ_f is the strain-relaxation time, w is the deflection of the ice sheet, ρ_w and ρ_i are the densities of water and ice, respectively, g is the acceleration of gravity, h is the thickness of the ice sheet, Φ is the fluid-motion potential, p is the external-load intensity, and H is the basin depth. The coordinate axes x and y lie in the plane of the ice plate with the x axis directed along the direction of motion of the load and the z axis directed upward.

The algorithm of solution of the above problem outlined in [2] allows one to study a wide range of problems connected with the motion of load over an ice sheet. One most important problem is calculation of the resonant velocity v_r upon rectilinear motion of a point force. To study the dependence of v_r on the basin depth H and the ice thickness h , we performed a series of calculations in which an ACS was modeled by the point force P equal to the ship weight.

A clamped rectangular-in-plan ice plate 1200 m long and 200 m wide was considered. The coordinate origin was located at its left edge and the x axis was directed to the right along the symmetry axis of the plate. At the initial moment, the force P was at rest and was applied at the point with the coordinates $x = 50$ m and $y = 0$; the corresponding static deflection of the plate was taken into account. The following

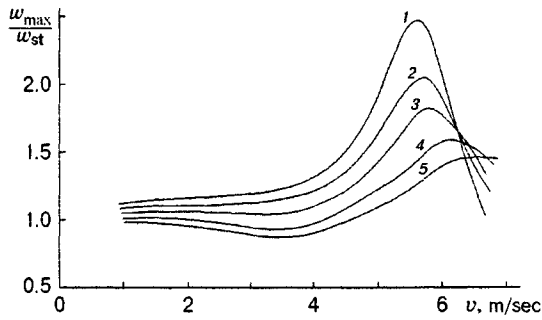


Fig. 1

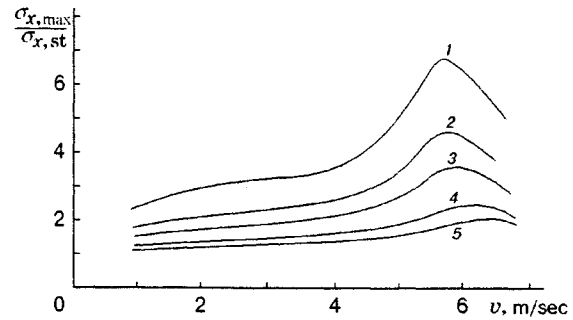


Fig. 2

law of motion of the load P was assumed: the load P begins to move along the x axis and, for the time τ_0 , attains the velocity v , at which it keeps on moving in the same direction.

In the calculations, the velocity of the load v , the basin depth H (3, 5, and 7 m), and the ice thickness h (0.3, 0.4, 0.5, 0.75, and 1.0 m) were varied.

The choice of the above values of H was motivated by the following reasons. As far as the author is aware, the problem of unsteady motion of an ACS over an ice sheet under shallow-water conditions has not yet been solved. However, this problem is of considerable interest, since icebreakers cannot be used in basins of small depth and, hence, the resonant method implemented by means of an ACS [1] is expedient.

The values of the other parameters of the problem were as follows: Young's modulus $E = 0.73 \cdot 10^{10}$ Pa, Poisson's ratio $\nu = 0.3$, $\rho_i = 900$ kg/m³, $\rho_w = 1000$ kg/m³, $\tau_f = 10$ sec, and $P = 0.4 \cdot 10^6$ N, which corresponds to a Voyager-type ACS. The discrete model of an ice plate was represented by a set of 16-D.O.F. square finite elements with side $a = 50$ m. The size of the time grid Δt [2] was taken to be 0.3125 sec, which ensured convergence of the finite-difference process. The static deflection of the ice plate was determined automatically at the beginning of execution of a computer code.

The stresses and deflections were determined for a steady stress-strain state, i.e., for the period of time where the steady strain pattern of the ice sheet shifts together with the load P . In this stage, the effects that arise owing to acceleration of the ship from the zero to the finite velocity v do not affect the stress-strain state; therefore, the acceleration time τ_0 was set to zero.

The calculations were performed in the following order. For a certain value of the velocity, the deflections were calculated at close moments of time from the initial moment to the moment the load reached the plate edge. From calculation results, we determined the time (initial and final positions of the load P) after which the process can be considered steady. Thereafter, the stresses and deflections were calculated for the specified value and smaller values of v . For example, if, for $v = 6.4$ m/sec, the motion is found to be steady when the load P passes through the point $x = 650$ m, one can assert that the motion at this point is also steady for, say, $v = 6$ m/sec or $v = 5$ m/sec; hence, the deflections and stresses can be calculated without verifying this fact additionally.

Figures 1 and 2 show the relative maximum deflection w_{\max}/w_{st} (w_{\max} is the maximum dynamic deflection and w_{st} is the maximum static deflection caused by the force P applied at the center of the ice plate) and the relative normal stresses $\sigma_{x,\max}/\sigma_{x,\text{st}}$ ($\sigma_{x,\max}$ and $\sigma_{x,\text{st}}$ are determined similarly to w_{\max} and w_{st}) versus v for $H = 3$ m and $h = 0.3, 0.4, 0.5, 0.75,$ and 1.0 m (curves 1–5, respectively). The character of the diagrams is the same for any depth considered, the only difference being that the maxima in the curves, which are located near the point $v = \sqrt{gH}$ in all the diagrams, are shifted toward larger values of v . The diagram of $\sigma_{y,\max}/\sigma_{y,\text{st}}$ versus v is similar to the diagram of $\sigma_{x,\max}/\sigma_{x,\text{st}}$.

Figure 3 shows the resonant velocity v_r versus the ice thickness h for basin depths of $H = 7, 5,$ and 3 m (curves 1–3, respectively).

The results imply the following conclusions.

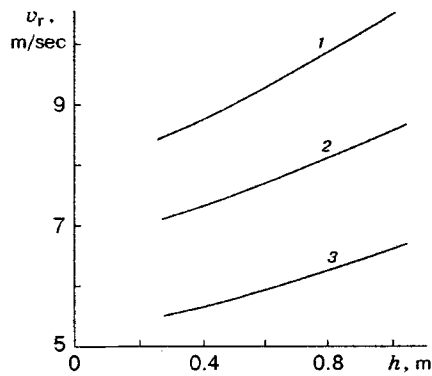


Fig. 3

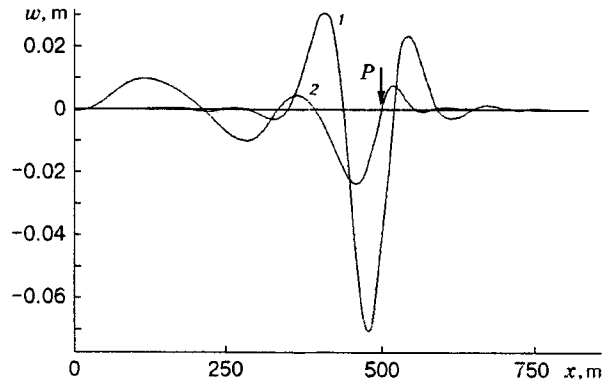


Fig. 4

1. The resonant velocity depends on the basin depth H and the ice thickness. One can see from Fig. 1 that the maximum of the relative deflection shifts toward larger values of v as the ice thickness h increases. For the values of H and h considered and small thickness of the ice, the velocity v_r that corresponds to the maximum deflection (resonant velocity) slightly exceeds the phase velocity of the gravity wave in water $v_0 = \sqrt{gH}$. The curves of v_r versus h have a small curvature in the range of the H and h values considered (Fig. 3).

2. For small values of H (3–5 m), the maxima in the curves of relative stresses (see Fig. 2) are shifted relative to the maxima of the deflections (see Fig. 1) toward larger values of v ; however, this shift is small and is approximately 2% of the resonant velocity v_r . For $H = 7$ m, the maximum deflections and stresses occur for almost the same velocity values.

3. The maximum values of the relative deflections that occur for v_r are close to each other at different values of H . For different H and the same thickness, the scatter in the values of w_{\max}/w_{st} amounts to 15–16% of the minimum relative deflection for given h . This is true for stresses as well.

It is of interest to study the effect of the velocity v on variation in the shape of the elastic surface of the ice plate. Figure 4 shows diagrams of the deflections along the x axis for $H = 3$ m and $h = 0.4$ m; curves 1 and 2 correspond to steady motion for $v = 5.6$ and 10 m/sec, respectively; the arrow shows the position of the load P . These diagrams are similar to the experimental curves obtained by Takizawa [4, 5], who revealed several characteristic stages of deflection. According to the classification proposed by Takizawa, the diagram for the resonant velocity $v = 5.6$ m/sec corresponds to a retarded transient regime: the maximum deflection occurs behind the load, the rear edge of the “deflection cup” at load is higher than the front edge, and the deflections are relatively large. The diagram for $v = 10$ m/sec can be related to the two-wave regime or the transition from the two-wave to the solitary-wave regime: the load tends to overtake the front wave; the waves that occur in front of the load are shorter than those behind the load; since the velocity exceeds the resonant value, the maximum deflection decreases.

Using the above algorithm, we solved the following problem, which is of practical significance: The point load P moves with constant velocity v over a clamped rectangular ice plate with a hole; the trajectory of load motion coincides with the plate symmetry axis x (Fig. 5). This situation can occur when an ACS crosses a bounded region of open water (mine, for example). So far, neither analytical nor numerical studies of the stress-strain state of ice have been performed in this formulation.

We consider some results of the solution of the above problem for the following data: the plate length $L = 1200$ m (Fig. 5), its width $B = 200$ m, $L_1 = 550$ m, the length and width of the hole (mine) 100 m, $P = 0.4 \cdot 10^6$ N, $E = 0.73 \times 10^{10}$ Pa, $\nu = 0.3$, the ice thickness $h = 0.5$ m, the basin depth $H = 5$ m, $\rho_i = 900$ kg/m³, $\rho_w = 1000$ kg/m³, $\tau_f = 10$ sec, and $v = 7$ m/sec. The load started to move from the point located 50 m from the left side of the plate. The acceleration time τ_0 was set to zero. The discrete model of a plate consisted of square finite elements with side $a = 50$ m.

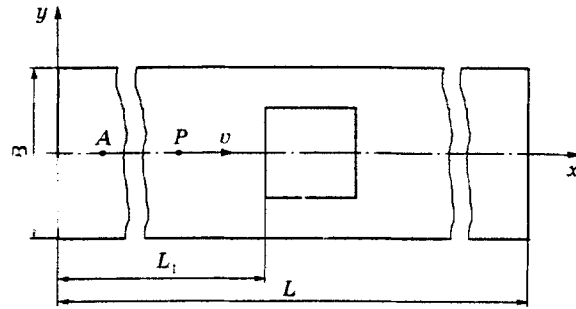


Fig. 5

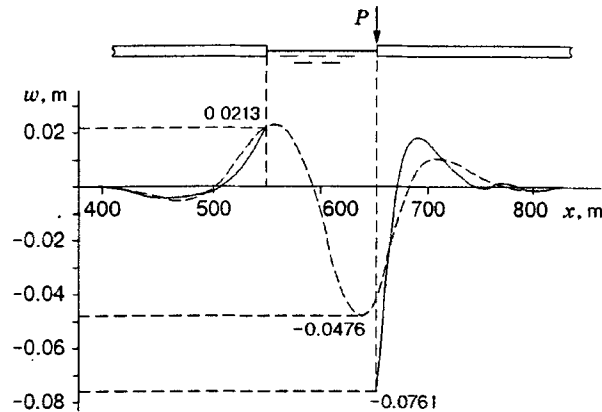


Fig. 6

The calculations show that the presence of a mine has little effect on the pattern of ice deflections until the load approaches the mine. The differences become pronounced after the load has crossed the mine: the maximum deflection increases significantly compared to the case of a plate without a hole. Figure 6 shows the diagram of deflections along the x axis at the moment the load P reaches the ice sheet after it has crossed the mine (the solid curve). For comparison, deflections in the plate without a hole (the dashed curve) were calculated, all other factors being the same.

It has been found that the maximum deflection is the greater, the lower the velocity. In comparison with the plate without a hole, the maximum deflection increases by approximately a factor of 1.5 and by more than twofold immediately after the load has crossed the mine for $v = 7$ m/sec (Fig. 6) and $v = 5$ m/sec, respectively. The increase in the deflection can be attributed to the fact that when the load crosses the mine, a gravity wave of larger amplitude compared to the flexural-gravity wave forms in the continuous ice field; this wave reaches the edge of the mine and intensifies the action of the load P .

REFERENCES

1. V. A. Zuev and V. M. Kozin. *The Use of Air-Cushion Ships in Ice Breaking* [in Russian]. Izd. Dal'nevost. Univ., Vladivostok (1988).
2. V. D. Zhestkaya, "Numerical solution of the problem of an ice sheet under a moving load." *Prikl. Mekh. Tekh. Fiz.*, **40**, No. 4, 243-248 (1999).
3. D. E. Kheisin, *Dynamics of an Ice Sheet* [in Russian], Gidrometeoizdat, Leningrad (1967).
4. T. Takizawa, "Deflection of a floating sea ice sheet induced by a moving load," *Cold Region Sci. Tech.*, **11**, 171-180 (1985).
5. R. J. Hosking, A. D. Sneyd, and D. W. Waugh, "Viscoelastic response of a floating ice plate to a steadily moving load," *J. Fluid Mech.*, **196**, 409-430 (1988).